JOURNAL OF VIROLOGY, July 2004, p. 7775–7783 Vol. 78, No. 14
0022-538X/04/$08.00+0 DOI: 10.1128/JVI.78.14.7775–7783.2004

Parvovirus B19-Induced Apoptosis of Hepatocytes

Brian D. Poole,[1,2] Yuory V. Karetnyi,[3]† and Stanley J. Naides[2]*

Integrated Biosciences Graduate Program[1] and Division of Rheumatology, Department of Medicine,[2] Pennsylvania State University College of Medicine, Hershey, Pennsylvania, and Division of Rheumatology, Department of Internal Medicine, The University of Iowa, Iowa City, Iowa[3]

Received 5 November 2003/Accepted 8 March 2004

Parvovirus B19 (B19 virus) can persist in multiple tissues and has been implicated in a variety of diseases, including acute fulminant liver failure. The mechanism by which B19 virus induces liver failure remains unknown. Hepatocytes are nonpermissive for B19 virus replication. We previously reported that acute fulminant liver failure associated with B19 virus infection was characterized by hepatocellular dropout. We inoculated both primary hepatocytes and the hepatocellular carcinoma cell line Hep G2 with B19 virus and assayed for apoptosis by using annexin V staining. Reverse transcriptase PCR analysis and immunofluorescence demonstrated that B19 virus was able to infect the cells and produce its nonstructural protein but little or no structural capsid protein. Infection with B19 virus induced means of 28% of Hep G2 cells and 10% of primary hepatocytes to undergo apoptosis, which were four- and threefold increases, respectively, over background levels. Analysis of caspase involvement showed that B19 virus-inoculated cultures had a significant increase in the number of cells with active caspase 3. Inhibition studies demonstrated that caspases 3 and 9, but not caspase 8, are required for B19 virus-induced apoptosis.

Parvovirus B19 (B19 virus) is the only parvovirus known to cause disease in humans. It is a small, single-stranded DNA virus that is transmitted in blood products or through aerosols and fomite contamination. B19 virus infection in children typically manifests as erythema infectiosum (fifth disease). Infection of adults frequently leads to arthropathy. In patients with chronic hemolytic anemias, such as sickle cell disease or hereditary spherocytosis, B19 virus infection causes transient aplastic crisis by destroying the erythroid precursor pool (34). Although these are the best-described clinical illnesses induced by B19 virus, the virus has been implicated in a wide spectrum of other illnesses.

Acute fulminant liver failure (AFLF) is a potentially fatal disease that may occur as a result of hepatic infection, toxic damage, or liver transplantation complications. Over one-third of idiopathic AFLF cases are accompanied by aplastic crisis (6). Langnas and colleagues demonstrated that a significant number of patients with AFLF associated with aplastic anemia had parvovirus B19 virus DNA in the native liver that was detectable by PCR (18). Karetnyi et al. demonstrated the presence of active B19 virus infection, as indicated by the presence of viral RNA, in AFLF associated with aplastic anemia. Interestingly, although RNA was detected, replicative forms of the viral genome were not, suggesting active infection without replication of the virus in these tissues (16). Hepatocytes express globoside, the receptor for B19 virus, and empty capsids will bind to extracts from liver tissue (9). Other diseases associated with B19 virus infection include arthropathy (32, 34), myocarditis (36), encephalitis (11), hepatitis (42), dermatomyositis (7), and scleroderma (22). Cooling and coworkers showed a link between tissues that are affected by B19 virus infection and the presence in those systems of globoside, the putative B19 virus receptor, and other neutral glycosphingolipids capable of binding B19 virus (9). This suggests that if the cellular receptor is present, B19 virus may cause damage even to cells that do not allow for the production of progeny virus.

B19 virus has been shown to productively replicate only in erythroid precursors, including fetal liver, isolated stem and bone marrow cells, and megakaryocytic leukemia cell lines maintained with erythropoeitin (3, 17, 29, 35). Upon infection of erythroid precursors, cell death occurs by apoptosis, probably caused by the viral nonstructural protein (NS1), which has been shown to induce apoptosis when transfected into erythroid cells (25, 26).

Although knowledge of the mechanisms through which B19 virus affects permissive cells is lacking, still less is understood about the interaction of B19 virus with cells that do not support viral replication. The block to productive infection in cell types other than erythroid precursors is not well understood, but aberrant splicing (4) or transcription (21) of the viral capsid proteins has been demonstrated. This block, however, does not affect production of the viral nonstructural protein (NS1) (4). B19 virus may be able to enter certain cells that express globoside and establish a restricted infection with production of NS1. Broad tropism for viral entry and NS1 production could explain the broad spectrum of disease associated with B19 virus infection.

In order to understand the process of B19 virus infection of nonpermissive cells in general and in AFLF specifically, we inoculated both primary hepatocytes and Hep G2 hepatocellular carcinoma cells with B19 virus. We analyzed the inoculated cells for production of NS1 and induction of apoptosis.

* Corresponding author. Mailing address: Division of Rheumatology, Department of Medicine, Pennsylvania State University College of Medicine, Milton S. Hershey Medical Center, 500 University Dr., Hershey, PA 17033. Phone: (717) 531-5384. Fax: (717) 531-8274. E-mail: snaides@psu.edu.

† Present address: Beckman Coulter, Inc., Chaska, MN 55318.

We further examined the pathways through which B19 virus infection induces apoptosis in these cells. This work directly demonstrates, for the first time, a cytopathic effect of B19 virus on liver cells. There is agreement that B19 virus DNA can be found in the livers of individuals with AFLF (12, 16, 18, 33, 50). The current debate centers on the relevance of the viral presence to a disease state. This work demonstrates a mechanism through which B19 virus can cause injury to liver tissue and is consistent with the demonstrated pathology of AFLF.

MATERIALS AND METHODS

Viruses and cell culture. Primary hepatocytes were obtained from BD Gentest and plated at 50% confluency onto collagen-coated 75-cm^2 flasks and four-well chamber slides. The donor was an adolescent Caucasian male whose cause of death was anoxia. Primary hepatocytes were maintained in Hepatozyme SFM medium (Invitrogen, Carlsbad, Calif.). Hep G2 cells were obtained from the American Type Culture Collection (Manassas, Va.). Cells were cultivated in hepatocyte wash buffer, a modified William's medium, with 10% fetal calf serum (Invitrogen). The cells were incubated at 37°C in a humidified 5% CO_2 incubator. Hep G2 cells were grown in eight-well LabTek II chamber slides (Nalge Nunc International, Rochester, N.Y.) for the annexin V staining and caspase 3 activity experiments and in 75-cm^2 tissue culture flasks (Fisher) for the reverse transcriptase PCR (RT-PCR) experiments.

Viremic serum from a patient with aplastic crisis was used as a B19 virus inoculant. The viral titer of this serum has been previously determined by PCR analysis to be 10^{12} viral genomes/ml (16).

Infection with B19 virus inoculants. Primary hepatocytes were inoculated with 1,000 viral genome equivalents/cell in Hepatozyme SFM serum-free medium. In order to improve detection of transcription and replication of B19 virus, we synchronized Hep G2 cells prior to inoculation by adding hydroxyurea to the cell culture medium at a final concentration of 2 mM. Cells were incubated with hydroxyurea for 40 h and then washed four times with wash buffer without serum. Synchronization was verified by staining cell nuclei with propidium iodide followed by DNA quantification using flow cytometry. After washing, the cells were inoculated with viremic serum diluted to a concentration of 1,000 viral particle per cell in Opti-MEM serum-free medium and incubated overnight. Cells were then washed and incubated with growth medium. The seemingly high multiplicity of infection (MOI) was presumably necessary because B19 virus is not able to replicate in liver cells and the primary inoculant is all of the virus that will be present, in contrast to the case for erythroid precursor cultures, in which a lower MOI can be used because of amplification through subsequent virus production. Furthermore, 1,000 viral genome equivalents per cell is not strictly an MOI but rather is a quantification of viral DNA. Due to the scarcity of B19 virus sources, it is necessary to utilize viremic serum as an inoculant, and serum contains inhibitors to B19 virus binding (2), further reducing the levels of infectious virions. This level of inoculation is physiologic in that viremic serum in a typical infection contains 10^{12} to 10^{15} virions per milliliter, which is comparable to the level in our inoculant (34).

RT-PCR. All steps involving RNA were performed in RNase-free plastic with RNase-free solutions. Hep G2 cells were grown to a concentration of 10^7 cells per flask, synchronized, and then inoculated with 10^{10} (10 μl of serum) viral particles in 5 ml of medium. Primary hepatocytes were inoculated 2 days after isolation with 10^{10} viral particles per flask as described for Hep G2 cells. At 3 days postinoculation, cells were trypsinized and centrifuged in medium at 200 × *g* for 5 min, and the medium was removed. The cells were then lysed in 2 ml of Trizol reagent (Invitrogen). Total RNA was extracted according to the manufacturer's directions. RNA was resuspended in 500 μl of RNase-free water (Invitrogen) and stored at −85°C until used. To rule out the possibility of false-positive signals due to DNA contamination, isolated RNA was treated with 10 U of RNase-free DNase (Roche, Indianapolis, Ind.) in RQ1 DNase buffer (Promega, Madison, Wis.) for 1 h at 37°C. An aliquot of extracted RNA was incubated with 10 U of DNase-free RNase (Roche) for 1 h at 37°C. RT-PCR was performed on 1 μg (pretreatment mass) of RNA from each condition by using the Superscript One Step RT-PCR with Platinum Taq system (Invitrogen). Extracted RNA was added to 47 μl of reaction buffer containing a 0.2 μM concentration of each primer and 1 μl of RT-Taq mix. To further ensure that a positive signal was not the result of DNA contamination, PCR was performed on one aliquot of DNase-treated RNA with Platinum Taq polymerase replacing the RT-Taq mix. For a positive PCR control, 1 μl of viremic serum was added in place of RNA in one tube. For detection of NS1 transcripts, the upstream primer consisted of the sequence 5′CAGTGGAAGTTTTCAAATTCAAAGT3′ and the downstream primer consisted of the sequence 5′ATGGCTTTTGCAGCTT C3′. For the detection of VP1/VP2 transcripts, the upstream and downstream primer sequences were 5′ATACTCAACCCCATGGAGA3′ and 5′TTCTGAT ATGGTTACAGTT3′, respectively, as previously described (16). All samples were incubated at 45°C for 30 min, denatured at 94°C for 2 min, and then subjected to 40 cycles of denaturation at 94°C for 30 s, annealing at 54°C for NS1 detection and at 52°C for VP1/VP2 detection for 2 min, and elongation at 72°C for 1 min. During the last 14 cycles, the elongation time was extended by 15 s per cycle. Products were analyzed on a 1.2% agarose submarine electrophoresis gel and stained with ethidium bromide.

Immunofluorescence. Hep G2 cells were grown on glass coverslips. They were synchronized with hydroxyurea and infected with 1,000 viral genome equivalents per cell. At 0, 8, 24, 48, 72, and 96 h postinfection, coverslips were removed and fixed in 4% paraformaldehyde. Cells were permeabilized with 0.2% Triton X-100 in phosphate-buffered saline (PBS) for 10 min and then washed. After blocking with 10% goat serum for 1 h, the anti-NS1 monoclonal antibody ParC-NS1 (a generous gift from Kazuo Sugamura, Tohoku University) (8) was diluted 1:200 in PBS and added to the coverslips. An isotype control antibody for mouse immunoglobulin G1 (IgG1) (Oncogene, Boston, Mass.) was diluted 1:200 and incubated with infected cells as a negative control. Coverslips were washed three times, and chicken anti-mouse IgG conjugated to Alexa-Fluor 488 (Molecular Probes, Eugene, Oreg.) was added to the coverslips. The coverslips were incubated with the secondary antibody for 1 h and then washed three times. To enhance detection, goat anti-chicken Ig conjugated to Alexa-Fluor 488 was incubated with the coverslips for 1 h and then the coverslips were washed three times. Fluorescence was viewed with a fluorescein isothiocyanate (FITC) filter set.

Annexin V staining. Virus-containing serum was diluted 1:1,000 in serum-free OPTI-MEM (Invitrogen) medium and incubated with either anti-B19 virus neutralizing antibody (NCL-PARVO; Novocastra Laboratories, Newcastle upon Tyne, United Kingdom) or an irrelevant isotype control antibody (mouse IgG1; PharMingen) at a 1:100 dilution for 60 min at 4°C. For UV-treated inoculants, virus-containing serum was diluted 1:1,000 and exposed to 2 J of UV irradiation/cm^2 in an Ultra-Lum UVC 508 UV cross-linker. Hep G2 cells grown in LabTek II chamber slides to a density of 2×10^5 cells/cm^2 were synchronized with hydroxyurea (2 mM) for 40 h. The cells were washed four times with serum-free medium and inoculated with 200 μl of NCL-PARVO or isotype control-treated diluted serum per well, for a final ratio of 1,000 viral genome equivalents per cell.

Primary hepatocytes were inoculated with 1,000 viral genome equivalents per cell or an equivalent amount of UV-irradiated inoculant. All cells were incubated for 3 days at 37°C in 5% CO_2. The growth medium was removed, and 500 μl of wash medium, 10 μl of medium binding reagent, and 1.25 μl of l annexin V-FITC (Oncogene) were added to each well. The slides were incubated for 15 min at room temperature, and then the medium was aspirated, growth chambers removed from the slides, and the cells were covered in binding buffer. Slides were immediately analyzed by fluorescence microscopy with a standard FITC filter set with a 450- to 490-nm excitation filter and a 515-nm long pass barrier filter. Green-staining cells were counted and compared to total cells to determine the percentage of annexin V-positive cells.

Caspase 3 activity. Hep G2 cells were grown, synchronized, and inoculated at a ratio of 1,000 viral genome equivalents per cell in eight-well LabTek II slides. At 3 days postinfection, the slides were washed and the medium and chambers were removed. Slides were covered with PhiPhiLux G_2D_2 caspase 3 fluorescent substrate (Oncogene) and incubated at 37°C for 45 min. The slides were then washed four times with PBS and examined immediately by fluorescence microscopy with a 528- to 553-nm excitation filter and a 600- to 660-nm barrier filter. Bright red cells were counted and divided by the total cells present in order to determine the percentage of cells positive for caspase 3 activity.

Caspase inhibition. Cells were inoculated as for annexin V staining, with the exception that the cell-permeative caspase 3 (and to a lesser extent caspase 6, 7, 8, and 10) inhibitor DEVD-FMK; the caspase 1, 4, and 5 inhibitor WEHD-FMK; the caspase 9 inhibitor LEHD-FMK; or the caspase 8 (and granzyme B) inhibitor IETD-FMK (Oncogene) was added to a final concentration of 10 μM 6 h before addition of the inoculant. Slides were also prepared with caspase inhibitors added to the medium, but without inoculation, in order to control for potential effects of the caspase inhibitors. Slides were incubated for 3 days and analyzed by annexin V staining as described above.

Statistical analysis. Significance was calculated by using the one-tailed Student *t* test. *P* values of less than 0.05 were considered significant.

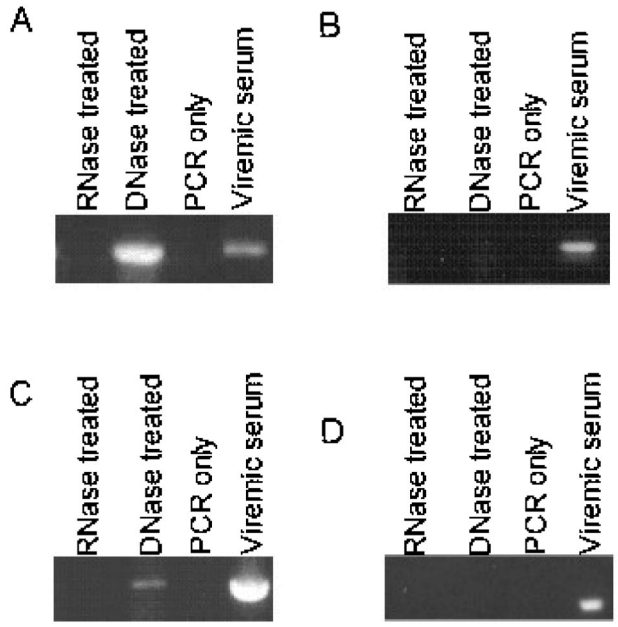

FIG. 1. B19 virus infects primary hepatocytes and Hep G2 cells, with production of NS1 but not structural protein RNA. RNA was isolated from inoculated primary hepatocytes and Hep G2 cells, and RT-PCR was performed to detect RNA transcripts for either the NS1 protein or the VP1/VP2 structural proteins. The specific NS1 amplification product was found at 403 bp, and the VP1/VP2 amplification product was found at 100 bp. (A) RNA from Hep G2 cells with primers specific for NS1. (B) RNA from Hep G2 cells with primers specific for VP1/VP2. (C) RNA from primary hepatocytes with primers specific for NS1. (D) RNA from primary hepatocytes with primers specific for VP1/VP2.

RESULTS

NS1 is expressed in Hep G2 cells in restricted infection. Because B19 virus is a DNA virus, RNA transcripts of its genes are found only after transcription of viral genes by the host cell. To test our hypothesis that B19 virus is able to establish a limited infection with the production of NS1, we performed RT-PCR analysis on RNA isolated from primary hepatocytes and Hep G2 cells inoculated with 1,000 viral genome equivalents per cell. We observed a specific 403-bp NS1 amplification product in the lanes representing the DNase-treated and positive control conditions but no band in the RNase-treated or PCR-only lanes. There was no detectable RNA for the structural protein VP1 or VP2 (Fig. 1). The lack of products under the PCR-only and RNase-treated conditions demonstrated that the template for the RT-PCR was RNA and not contaminating DNA. The presence of viral RNA indicated that despite being unable to replicate in Hep G2 cells, the virus was able to enter cells and utilize cellular machinery to produce transcripts for NS1. The absence of VP1 or VP2 transcripts demonstrated that infection is restricted in hepatocytes in vitro, with no production of progeny virions.

Immunofluorescence staining for NS1 by using a multifunctional anti-NS1 monoclonal antibody (8) demonstrated bright punctate nuclear staining in 36% of infected cells by 48 h postinfection. It was not possible to quantitate the total number of cells infected by using NS1 staining because the anti-NS1 monoclonal antibody available stained cytoplasm nonspecifically. Therefore, we could not differentiate between nonspecific staining and NS1 expression in the cytoplasm. Nuclear staining, however, was specific and was not seen in uninfected cells. Hoechst 33342 staining of the nuclei allowed localization of the NS1 signal to the nucleus, as seen in merged images of NS1 and nuclear staining. No staining was seen in primary antibody isotype control-stained cells (Fig. 2). The presence of NS1 protein in the nucleus indicated that translation of NS1 transcripts and translocation of NS1 protein to the nucleus occurs in Hep G2 cells, and therefore the transcripts seen in the RT-PCR assays are functional.

B19 virus infection induces apoptosis in liver cells. After confirming that infection of liver cells occurred, we next examined the effect of infection on the host cell. To determine whether B19 virus infection induced apoptosis, we inoculated primary hepatocytes and Hep G2 cells with 1,000 viral genome equivalents per cell and analyzed them for apoptosis by annexin V-FITC staining at 1, 2, 3, and 4 days postinfection. Annexin V binds specifically to phosphatidylserine (PS). PS is normally found only on the inner leaflet of the cell membrane, but during the early stages of apoptosis, this polarity is lost and PS can be detected on the external surface of the cell. Apoptosis in inoculated Hep G2 cells was maximal at 3 days postinfection (Fig. 3). Apoptosis in inoculated primary hepatocytes was not seen until day 3, while uninoculated primary hepatocytes remained viable for at least 5 days. In subsequent experiments, cells were incubated for 3 days. To control for the effects of serum in the inoculant and the effects of viral capsid protein and DNA, we mock inoculated cells with nonviremic serum (Sigma), NCL-PARVO neutralized viremic serum, or UV-irradiated viremic serum. Examination of stained cells demonstrated that approximately threefold more cells underwent apoptosis in the inoculated cultures than in the mock-inoculated cultures. In Hep G2 cultures, 28% of cells in inoculated cultures versus 10% mock-inoculated cells underwent apoptosis. Pretreatment of viral inoculants with the neutralizing anti-B19 virus monoclonal antibody NCL-PARVO or UV irradiation of the inoculant reduced apoptosis in Hep G2 cells to 7 and 12% of cells, respectively. Approximately threefold more primary hepatocytes underwent apoptosis when inoculated with B19 virus (24%) than when inoculated with UV-irradiated B19 virus (7.6%) (Fig. 4). The apoptosis induced by B19 virus infection was dose dependent, with increasing viremic serum concentrations in the inoculant resulting in increasing cell death (Fig. 5).

B19 virus-induced apoptosis requires caspases 3 and 9 but not caspase 8. Apoptosis proceeds through the activation of a family of cysteine proteases called caspases. Caspase 3 is a downstream caspase that plays a key role in cleavage of nuclear proteins and the activation of other caspase family members. Caspase 3 has been implicated in apoptosis induced by B19 virus in permissive cells and in apoptosis induced by the Rep 78 protein of adeno-associated virus, a nonpathogenic human parvovirus (41). We examined caspase 3 activation in Hep G2 cells by using the cell-permeative fluorescent caspase 3 substrate PhiPhiLux G_2D_2. If caspase 3 is active in the cell, the substrate is cleaved and trapped intracellularly so that it can be detected by fluorescence microscopy. In inoculated Hep G2 cells, over twice as many inoculated cells (44.6%) as mock-

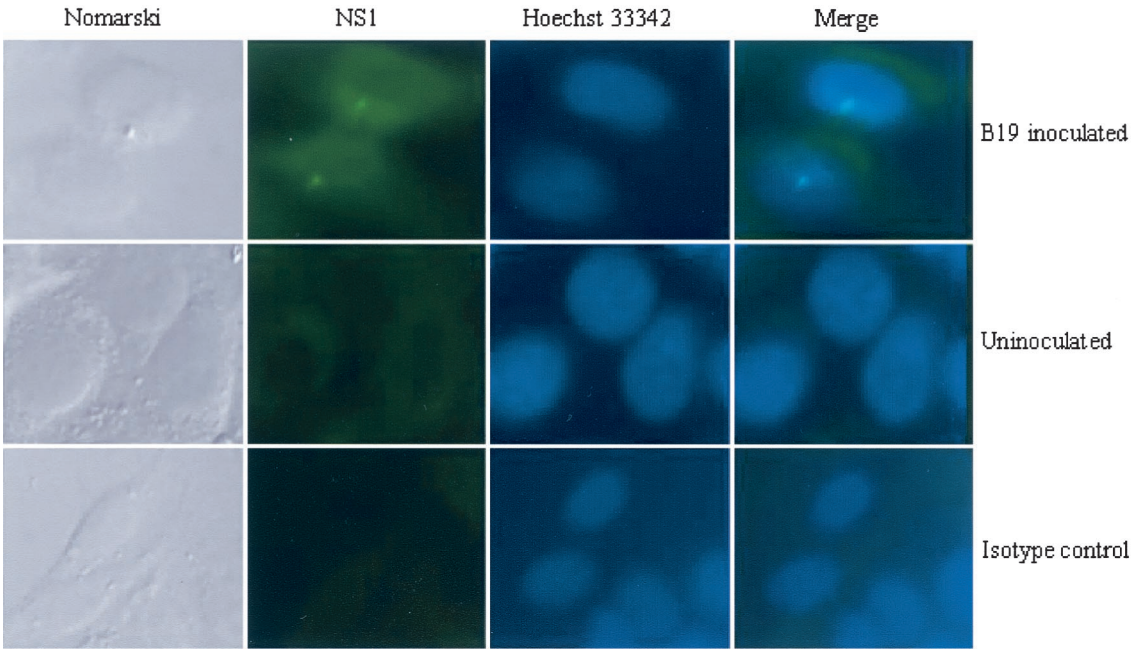

FIG. 2. B19 virus infection results in production of NS1 protein. Immunofluorescence reveals NS1 protein as nuclear punctuate staining in the infected cells but not in the uninfected cells or on the isotype control-treated slides. Hoechst 33342-stained nuclei are also shown. NS1 staining was seen in 36% of cells and demonstrates functionality of NS1 transcripts. Merged images of NS1 and Hoechst 33342 staining demonstrated NS1 localization to the nucleus.

inoculated cells (20.6%) were positive for caspase 3 activity (Fig. 6). In this system, incomplete removal of uncleaved substrate despite washing leads to a higher background for mock-inoculated cells in caspase 3 assays (Fig. 6B) (20.6%) than in annexin V staining assays (Fig. 4C) (10%). We used annexin V staining for apoptosis detection because of its greater specificity for apoptosis, but we used PhiPhiLux substrate staining to demonstrate caspase 3 activity.

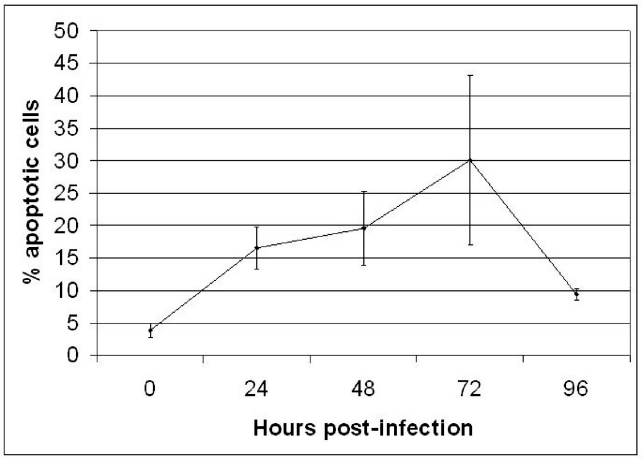

FIG. 3. Time course of B19 virus-induced apoptosis of hepatocytes. Hep G2 cells were synchronized and infected with 1,000 viral genome equivalents/cell. Apoptosis was assayed by annexin V staining at 1, 2, 3, and 4 days postinfection. Apoptosis increases up to 3 days postinfection. After 3 days, it abruptly declines. Error bars indicate standard deviations.

In order to determine whether caspase 3 activation was required for B19 virus-induced apoptosis, we inhibited caspase 3 with DEVD-FMK, a cell-permeative selective caspase 3 inhibitor. We assayed for apoptosis in B19 virus-inoculated Hep G2 cells by using annexin V staining. DEVD-FMK blocked apoptosis by B19 virus, returning the number of annexin V positive cells to background levels (5.6% in Hep G2 cells and 7.3% in primary hepatocytes) (Fig. 7). DEVD-FMK also inhibits caspases 6, 7, 8, and 10, but to a lesser extent than it does caspase 3. Inhibitors of caspases 6 or 7 that do not also inhibit caspase 3 are not available. Caspases 6 and 7 are activated downstream from caspase 3. The PhiPhiLuxG2D2 substrate experiments described above directly show caspase 3 activation. Inhibitors to caspase 10 alone are not available.

There are multiple apoptotic pathways through which a cell can die, and these pathways are regulated by different caspases that lead to downstream activation of caspase 3. The tumor necrosis factor (TNF) family member-induced cell death pathways activate caspase 8 (1, 30). Caspase 8 is the first of the caspases activated by this "extrinsic" pathway, and it transduces extracellular signals for apoptosis. The "intrinsic" pathways that induce apoptosis, for example, in response to DNA damage or growth factor withdrawal, are transduced through the mitochondria and utilize caspase 9. Previous studies have suggested that B19 virus infection can sensitize erythroid cells to TNF-induced apoptosis (45), a pathway that would proceed through caspase 8 (1, 30). Caspase 8 directly activates caspase 3, which further transduces the apoptotic cascade leading to cell death (40, 46, 47).

We inhibited caspase 8 and caspase 9 with, respectively, IETD-FMK and LEHD-FMK, irreversible cell-permeative se-

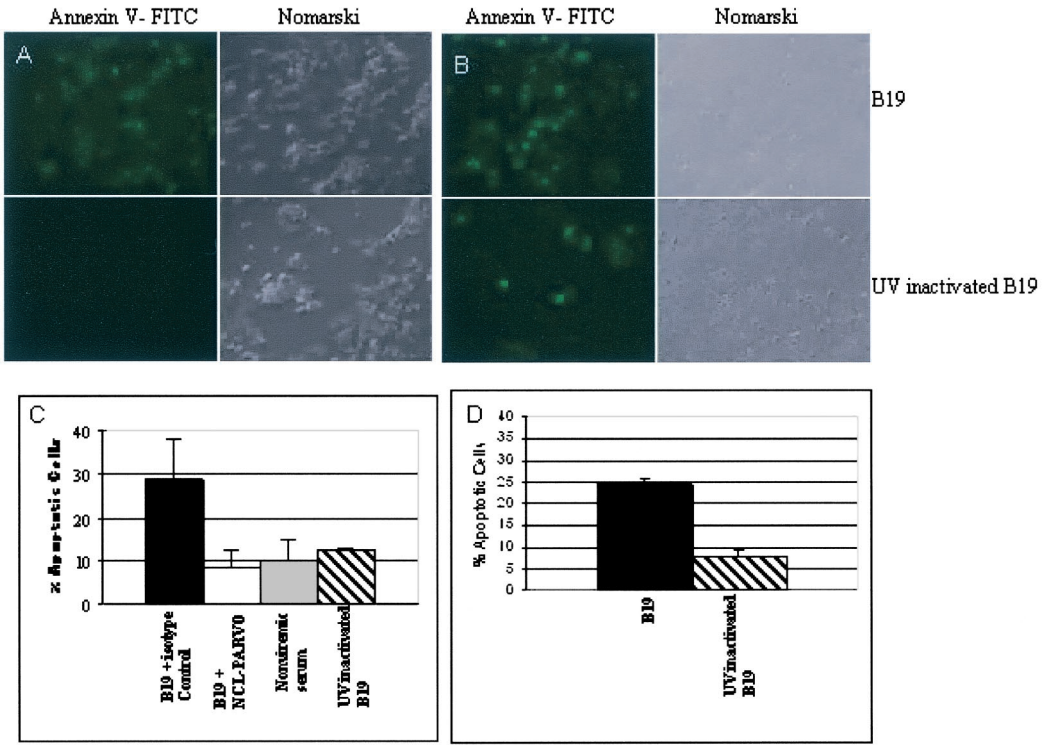

FIG. 4. Hepatocytes undergo apoptosis in response to infection by B19 virus. (A and B) Annexin V staining shows increased numbers of apoptotic cells in the inoculated cultures (top row) compared to mock-inoculated cultures (bottom row). (A) Hep G2 cells. (B) Primary hepatocytes. (C) Effect of neutralizing antibody or UV irradiation of B19 virus on apoptosis of Hep G2 cells. Infection with B19 virus plus isotype control antibody allows apoptosis at a much higher rate than inoculation with B19 virus neutralized with the antibody NCL-PARVO, mock inoculation with nonviremic serum ($P < 0.005$), or inoculation with UV-irradiated B19 virus ($P < 0.04$). (D) Primary hepatocytes inoculated with B19 virus undergo significantly more apoptosis than those inoculated with UV-irradiated B19 virus ($P < 0.008$). Error bars indicate standard deviations.

lective caspase inhibitors. LEHD-FMK also inhibits caspases 4 and 5, but to a lesser extent than caspase 9. To control for inhibition of caspases 4 and 5, we treated cells with WEHD-FMK, a caspase inhibitor that blocks activity of caspases 1, 4, and 5, but not 9 (31). The cells were inoculated with B19 virus after 6 h of incubation with caspase inhibitors. Hep G2 cells pretreated with WEHD-FMK or IETD-FMK demonstrated no decrease in apoptosis. In contrast, pretreatment with DEVD-FMK or LEHD-FMK significantly decreased B19 virus-induced Hep G2 cell apoptosis, with a return to background levels (Fig. 7A). In primary hepatocytes, there was a slight decrease in apoptosis noted after all caspase pretreatments compared to inoculation alone (Fig. 4C), but there was a significantly larger decrease, with return to background levels, in the DEVD-FMK- and LEHD-FMK-pretreated cells (Fig. 7B). In order to verify that the caspase 8 inhibitor IETD-FMK was functional at the concentrations used, we demonstrated that IETD-FMK was able to reduce apoptosis in Hep G2 cells treated with an anti-Fas antibody (data not shown). Therefore, the lack of IETD-FMK-mediated inhibition of apoptosis in the B19 virus studies was not due to lack of activity of the inhibitor. Further, in the absence of infection, none of the inhibitors affected apoptosis (Fig. 7). These findings indicate that in hepatocytes, B19 virus induces apoptosis through a caspase 9-dependent, caspase 8-independent pathway. The implication is that the TNF receptor family is not necessary for apoptosis in B19 virus-inoculated cells and that apoptosis proceeds through an intrinsic pathway, possibly as a result of DNA damage or an as-yet-undiscovered process.

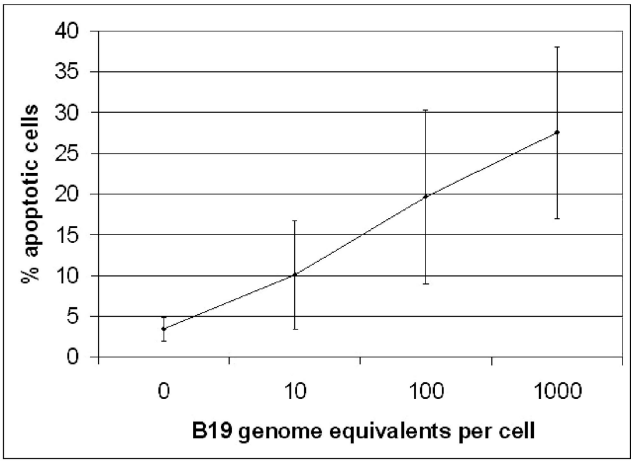

FIG. 5. B19 virus-induced apoptosis is infectious dose dependent. Increasing virus-to-cell ratios leads to increased apoptosis as measured by annexin V staining in Hep G2 cells. Error bars indicate standard deviations.

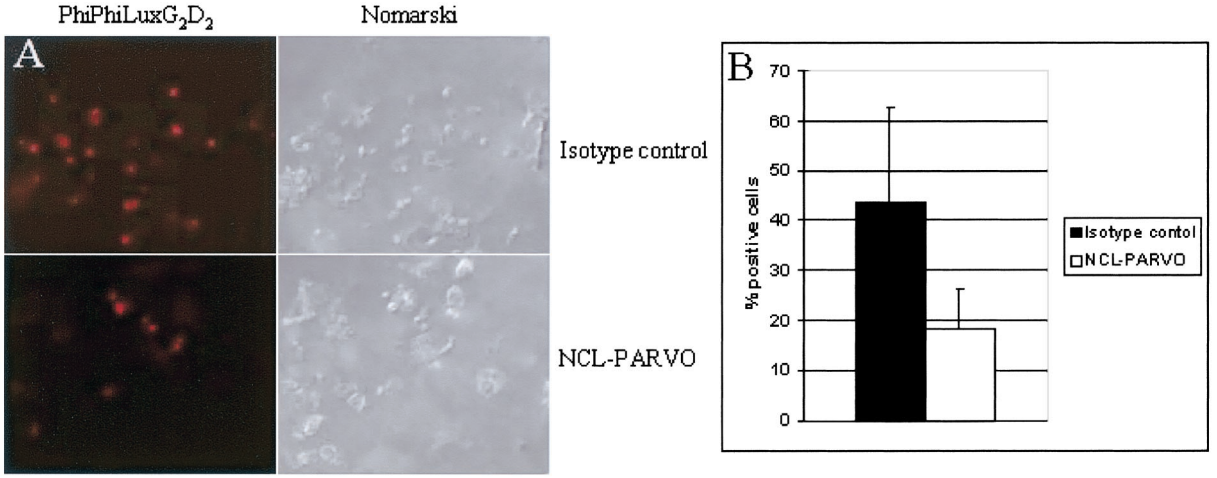

FIG. 6. Caspase 3 activity is increased in inoculated Hep G2 cells compared to mock inoculated cells. (A) Red cells are positive for caspase 3 activity. Top row, mock-inoculated cells; bottom row, inoculated cells. Left column, fluorescence of caspase 3-activated PhiPhiLuxG_2D_2 substrate; right column, Nomarski differential interference contrast. (B) Effect of neutralizing antibody to B19 virus on quantification of the number of cells with active caspase 3. Cells incubated with viremic serum neutralized with NCL-PARVO antibody show a lower percentage of cells with active caspase 3 than cells inoculated with viremic serum and an irrelevant isotype control antibody ($P = 0.006$). Error bars indicate standard deviations.

DISCUSSION

B19 virus was discovered in a pool of serum samples being tested for hepatitis B virus (10). Numerous reports and studies have subsequently implicated B19 virus in pathological processes of the liver, including posttransplantation liver dysfunction (19, 42), hepatitis (14, 23, 37, 38, 48, 51), and fulminant liver failure (16, 18, 33, 44, 49). Our data demonstrate that B19 virus is capable of infecting and inducing apoptosis in both primary hepatocytes and a liver-derived cell line. This is the first report demonstrating the cytopathic effect of B19 virus on hepatocytes, and it provides an explanation for liver-associated hepatic disease.

Multiple studies have shown persistence of B19 virus DNA in various tissues, including synovium (15, 43), skin (22), and liver (12, 18). The significance of the presence of latent B19 virus DNA in these tissues is not well understood. Viral DNA persistence may occur without causing deleterious effects on the cell. The long-term persistence of viral DNA renders demonstration of the association of a virus with disease more difficult, since latent viral DNA can often be found in individuals without disease activity. Two reports have disputed the association of B19 virus with AFLF. Eis-Hübinger and colleagues detected B19 virus DNA in explanted livers from 17 of 43 individuals (40%) undergoing orthotopic liver transplantation for chronic liver disease of defined etiologies (12). This prevalence of B19 virus DNA was somewhat higher than that in our control group of patients undergoing orthotopic liver transplantation for chronic liver disease (16), but we hypothesize that the difference represents the older age of the population in the study by Eis-Hübinger et al. and the opportunity to acquire B19 virus infection with age. In addition, the study by Eis-Hübinger and colleagues did not include a group of patients with AFLF for comparison. While we detected a B19 virus DNA prevalence of 18% in explanted livers from patients with chronic liver disease, the prevalence was 83% (five of six) in explanted livers from patients with AFLF and aplastic anemia. In a group of 10 patients with AFLF but without aplastic anemia, 3 of 4 (75%) with cryptogenic AFLF had B19 virus DNA detected in explanted livers, but only 1 of 6 (17%) with AFLF of known cause had B19 virus DNA (16).

Using nested PCR, Wong and colleagues reported no difference in prevalence of liver B19 virus DNA in fulminant hepatitis (35%) versus hepatitis B or C virus infections (33%). However, their data showed a significant difference when fulminant hepatitis (35%) was compared to biliary atresia (5%) (50). In their report, liver samples from individuals with anemia associated with chronic hepatitis had a low prevalence (9%) of B19 virus DNA. However, their hepatitis-associated anemia patients may not be comparable to our AFLF patients, because they included individuals who developed aplastic anemia within 6 months of hepatitis onset, whereas our patients were diagnosed with aplastic anemia at a median of 4 weeks after the onset of hepatitis, with the aplasia seen before transplantation in the majority (6). Differences in the time of onset of aplasia in these two reports suggests that the two studies identified different patient populations with differing mechanisms of liver disease and aplasia. Further, rather than arguing against a role for B19 virus in liver disease, their data suggest that B19 virus may play a role in accelerating the course of hepatitis B and C liver disease and/or that superinfection with hepatitis B or C virus may play a role in B19 virus expression in liver. Interestingly, B19 virus transcription is enhanced in the presence of a superinfection with adenovirus (39). The suggestion by Eis-Hübinger et al. (12) that B19 virus may persist in liver parallels the findings of B19 virus persistence in synovia from healthy adults and in bone marrow from adults with chronic B19 virus arthritis (13, 43).

In order to demonstrate the relevance of B19 virus to disease, it is necessary to delineate the effects of the virus on the liver. Finding viral DNA in healthy individuals does not eliminate the virus as a candidate causative agent. Virus could remain latent for a period of time before reactivation or a

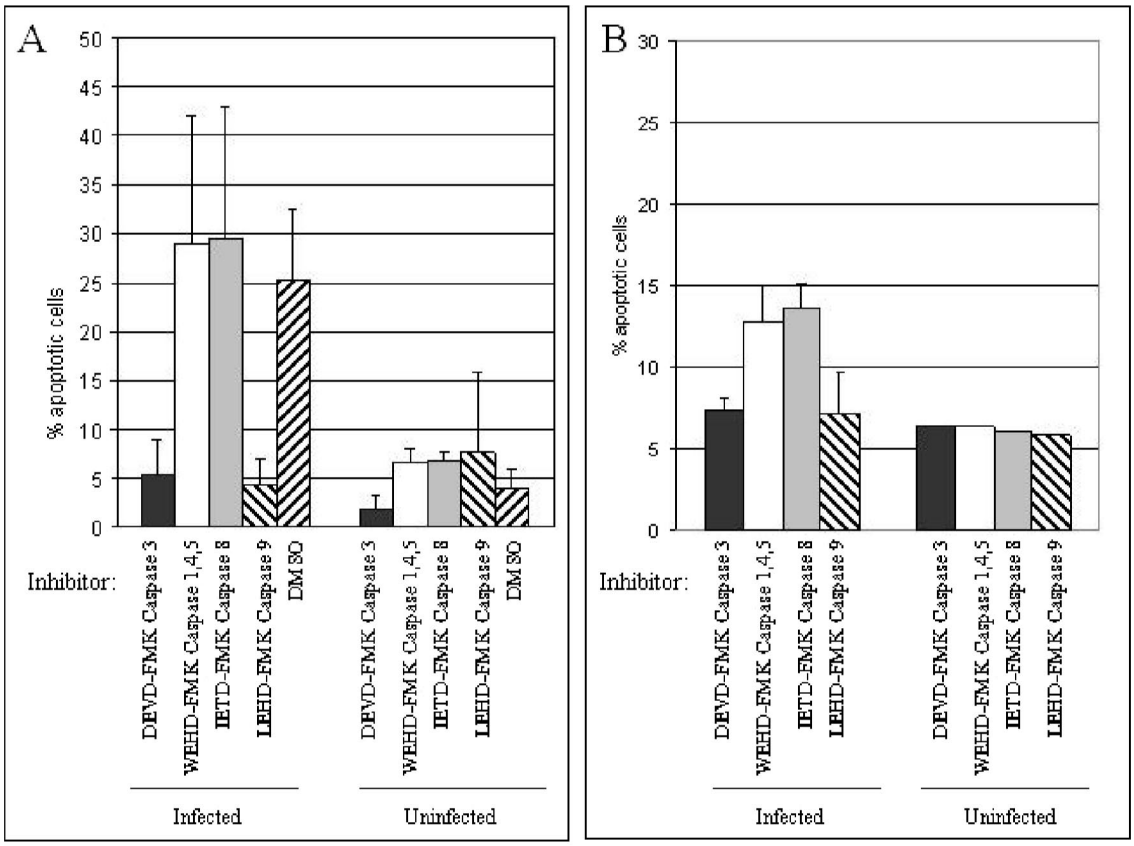

FIG. 7. Apoptosis induced by B19 virus is dependent on caspase 3 and 9 activity but not on caspase 8 activity. Cells were inoculated or mock inoculated in the presence of the caspase inhibitor IETD-FMK (inhibits caspase 8), DEVD-FMK (inhibits caspase 3 and to a lesser extent caspases 6, 7, 8, and 10), WEHD-FMK (inhibits caspases 1, 4, and 5), or LEHD-FMK (inhibits caspases 9 and to a lesser extent caspases 4 and 5). (A) Caspase inhibition with DEVD-FMK and LEHD-FMK significantly decreased apoptosis in inoculated Hep G2 cells ($P < 0.001$ and $P < 0.001$, respectively), while WEHD-FMK and IETD-FMK showed no significant decrease in apoptosis. (B) In primary hepatocytes, DEVD-FMK and LEHD-FMK also inhibited apoptosis to a significant extent, returning the levels of apoptosis to background ($P < 0.002$ and $P < 0.01$, respectively). In the absence of infection, the inhibitors did not demonstrate any effects on apoptosis. Error bars indicate standard deviations.

second hepatic insult leads to clinical liver disease. Failure to detect anti-B19 virus IgM antibody in our previously described patients with AFLF and B19 virus DNA may represent reactivation of latent infection (18). Similarly, B19 virus DNA but not capsid protein was detected in myocardium from an infant with fulminant myocarditis (36). The factors that may induce NS1 expression in latent B19 virus infection remain to be determined.

The present study goes a step beyond merely finding DNA to demonstrate that B19 virus is able to infect liver cells, with subsequent production of NS1 and induction of apoptosis. These findings establish that B19 virus is not simply a passenger in liver cells but has the capacity to cause cell death. The apoptosis of hepatocytes in vitro upon inoculation with B19 virus is consistent with the dropout of hepatocytes seen in patients with AFLF and associated aplastic anemia (18). These findings reinforce the previously demonstrated association of B19 virus with AFLF and define a mechanistic paradigm to explain how B19 virus may cause this disease. Furthermore, our results suggest the possibility that B19 virus disease manifestations in nonerythroid tissues, such as arthropathy (32), myocarditis (36), scleroderma (22), dermatomyositis (7), may also be a result of B19 virus restricted infection of nonpermissive cells.

A recent report by Morita and colleagues demonstrated that the B19 virus-induced processes of cell cycle arrest at G_2 phase and of apoptosis were not coupled in erythroid progenitors (27, 28). Our work supports these findings, because primary hepatocytes are nonreplicating cells but B19 virus still induces apoptosis. Therefore, B19 virus induction of apoptosis in hepatocytes does not appear to require cell cycle events. In contrast, the rodent H1 parvovirus replicates and induces apoptosis in rapidly cycling human hepatoma cell lines but not in noncycling human primary hepatocytes (24). H1 is sufficiently different from B19 virus in that B19 virus did not replicate in the Hep G2 hepatoma cell line.

Our study suggests a mechanism by which B19 virus induces apoptosis. Our data indicate that B19 virus-induced apoptosis proceeds through a caspase 3-dependent pathway. Caspase 8 activity is not necessary for B19 virus-induced apoptosis, suggesting that the action of B19 virus on Hep G2 cells is a result of an apoptotic pathway initiated within the infected cell rather than as a result of an exogenous signal of a TNF receptor family member. A candidate molecule for affecting apoptosis

in Hep G2 cells is the B19 virus nonstructural protein NS1, a multifunctional protein with endonuclease, helicase, nucleotide triphosphate binding, and transactivating activities (25, 26). We demonstrated expression of NS1 RNA but not VP1/VP2 transcripts. Further, UV-irradiated virus did not induce apoptosis. While Lindton and colleagues reported that empty recombinant B19 virus capsids inhibit erythroid colony formation, they did not examine apoptosis induction (20). Inhibition may have been caused by agglutination of erythroid cells by the capsid through the B19 virus receptor. B19 virus is known to hemagglutinate erythrocytes through binding a B19 virus receptor, globoside (2). Our results suggest that NS1 transcription is important in cell death. In nonhepatocyte systems, NS1 transfection has been shown to be cytotoxic (5, 25, 26). We demonstrated NS1 nuclear staining in 36% of infected Hep G2 cells by 48 h postinfection. Demonstration of the presence of NS1 protein in the nucleus and the similarity in the percentages of cells staining for nuclear NS1 and cells undergoing apoptosis suggested that B19 virus causes apoptosis of hepatocytes through NS1 expression. These finding suggest a role for NS1 in B19 virus-induced apoptosis of human hepatocytes. Further studies will be required to determine possible mechanisms of NS1-induced apoptosis.

ACKNOWLEDGMENT

This work was supported in part by the Arthritis Foundation Central Pennsylvania Chapter.

REFERENCES

1. **Boldin, M. P., T. M. Goncharov, Y. V. Goltsev, and D. Wallach.** 1996. Involvement of MACH, a novel MORT1/FADD-interacting protease, in Fas/Apo-1 and TNF receptor-induced cell death. Cell **85:**803–815.
2. **Brown, K. E., and B. J. Cohen.** 1992. Haemagglutination by parvovirus B19. J. Gen. Virol. **73:**2147–2149.
3. **Brown, K. E., J. Mori, B. J. Cohen, and A. M. Field.** 1991. In vitro propagation of parvovirus B19 in primary foetal liver culture. J. Gen. Virol. **72:**741–745.
4. **Brunstein, J., M. Söderlund-Venermo, and K. Hedman.** 2000. Identification of a novel RNA splicing pattern as a basis of restricted cell tropism of erythrovirus B19. Virology **247:**284–291.
5. **Caillet-Fauquet, P., M. Perros, A. Brandenburger, P. Spegelaere, and J. Rommelaere.** 1990. Programmed killing of human cells by means of an inducible clone of parvoviral genes encoding non-structural proteins. EMBO J. **9:**2989–2995.
6. **Cattral, M. S., A. Langnas, R. Markin, D. Antonson, T. Heffron, I. Fox, M. Sorrell, and B. Shaw, Jr.** 1994. Aplastic anemia after liver transplantation for fulminant liver failure. Hepatology **20:**813–818.
7. **Chevrel, G., A. Calvet, V. Belin, and P. Miossec.** 2000. Dermatomyositis associated with the presence of parvovirus B19 DNA in muscle. Rheumatology **39:**1037–1039.
8. **Chisaka, H., E. Morita, K. Tada, N. Yaegashi, K. Okamura, and K. Sugamura.** 2003. Establishment of multifunctional monoclonal antibody to the nonstructural protein, NS1, of human parvovirus B19. J. Infect. **47:**236–242.
9. **Cooling, L. L., T. A. W. Koerner, and S. J. Naides.** 1995. Multiple glycosphingolipids determine the tissue tropism of parvovirus B19. J. Infect. Dis. **172:**1198–1205.
10. **Cossart, Y. E., A. M. Field, B. Cant, and D. Widdows.** 1975. Parvovirus-like particles in human sera. Lancet **i:**72–73.
11. **Druschky, K., J. Walloch, J. Heckmann, B. Schmidt, H. Stefan, and B. Neundörfer.** 2000. Chronic parvovirus B-19 meningoencephalitis with additional detection of Epstein-Barr virus DNA in the cerebrospinal fluid of an immunocompetent patient. J. Neurovirol. **6:**418–422.
12. **Eis-Hübinger, A., U. Reber, T. Abdul-Nour, U. Glatzel, H. Lauschke, and U. Pütz.** 2001. Evidence for persistence of parvovirus B19 DNA in livers of adults. J. Med. Virol. **65:**395–401.
13. **Foto, F., K. G. Saag, L. L. Scharosch, E. J. Howard, and S. J. Naides.** 1993. Parvovirus B19-specific DNA in bone marrow from B19 arthropathy patients: evidence for B19 virus persistence. J. Infect. Dis. **167:**744–748.
14. **Granot, E., H. Miskin, and M. Aker.** 2001. Monoclonal anti-CD52 antibodies: a potential mode of therapy for parvovirus B19 hepatitis. Transplant. Proc. **33:**2151–2153.
15. **Hokynar, K., J. Brunstein, M. Söderlund-Venermo, O. Kiviluoto, E. Partio, Y. Konttinen, and K. Hedman.** 2000. Integrity and full coding sequence of B19 virus DNA persisting in human synovial tissue. J. Gen. Virol. **81:**1017–1025.
16. **Karetnyi, Y. V., P. Beck, R. Markin, A. Langnas, and S. Naides.** 1999. Human parvovirus B19 infection in acute fulminant liver failure. Arch. Virol. **144:**1713–1724.
17. **Kurtzman, G., P. Gascon, M. Caras, B. Cohen, and N. S. Young.** 1998. B19 parvovirus replicates in circulating cells of acutely infected patients. Blood **71:**1448–1454.
18. **Langnas, A., R. Markin, M. Cattral, and S. Naides.** 1995. Parvovirus B19 as a possible causative agent of fulminant liver failure and associated aplastic anemia. Hepatology **22:**1661–1665.
19. **Lee, P., C. Hung, Y. Lin, J. Wang, M. Jan, and H. Lei.** 2002. A role for chronic parvovirus B19 infection in liver dysfunction in renal transplant recipients. Transplantation **73:**1635–1639.
20. **Lindton, B., T. Tolfvenstam, O. Norbeck, L. Markling, O. Ringden, M. Westgren, and K. Broliden.** 2001. Recombinant parvovirus B19 empty capsids inhibit fetal hematopoietic colony formation in vitro. Fetal Diagn. Ther. **16:**26–31.
21. **Liu, J. M., S. W. Green, T. Shimada, and N. S. Young.** 1992. A block in full-length transcript maturation in cells nonpermissive for B19 parvovirus. J. Virol. **66:**4686–4692.
22. **Magro, C. M., M. R. Dawood, and A. N. Crowson.** 2000. The cutaneous manifestations of human parvovirus B19 infection. Hum. Pathol. **31:**488–496.
23. **Metzman, R., A. Anand, P. A. DeGiulio, and A. S. Knisely.** 1989. Hepatic disease associated with intrauterine parvovirus B19 infection in a newborn premature infant. J. Pediatr. Gastroenterol. Nutr. **9:**112–114.
24. **Moehler, M., B. Blechacz, N. Weiskopf, M. Zeidler, W. Stremmel, J. Rommelaere, P. R. Galle, and J. J. Cornelis.** 2001. Effective infection, apoptotic cell killing and gene transfer of human hepatoma cells but not primary hepatocytes by parvovirus H1 and derived vectors. Cancer Gene Ther. **8:**158–167.
25. **Moffatt, S., N. Yaegashi, K. Tada, N. Tanaka, and K. Sugamura.** 1998. Human parvovirus B19 nonstructural protein induces apoptosis in erythroid lineage cells. J. Virol. **72:**3018–3028.
26. **Momoeda, M., S. Wong, M. Kawase, N. S. Young, and S. Kajigaya.** 1994. A putative nucleoside triphosphate-binding domain in the nonstructural protein of B19 parvovirus is required for cytotoxicity. J. Virol. **68:**8443–8446.
27. **Morita, E., A. Nakashima, H. Asao, H. Sato, and K. Sugamura.** 2003. Human parvovirus B19 nonstructural protein (NS1) induces cell cycle arrest at G_1 phase. J. Virol. **77:**2915–2921.
28. **Morita, E., K. Tada, H. Chisaka, H. Asao, H. Sato, N. Yaegashi, and K. Sugamura.** 2001. Human parvovirus B19 induces cell cycle arrest at G_2 phase with accumulation of mitotic cyclins. J. Virol. **75:**7555–7563.
29. **Munshi, N. C., S. Zhou, M. J. Woody, D. A. Morgan, and A. Srivastava.** 1993. Successful replication of parvovirus B19 in the human megakaryocytic leukemia cell line MB-02. J. Virol. **67:**562–566.
30. **Muzio, M., A. M. Chinnaiyan, F. C. Kischkel, K. O'Rourke, A. Shevchenko, J. Ni, C. Scaffidi, J. D. Bretz, M. Zhang, R. Gentz, M. Mann, P. H. Krammer, M. E. Peter, and V. M. Dixit.** 1996. FLICE, a novel FADD-homologous ICE/CED-3-like protease, is recruited to the CD95 (Fas/APO-1) death-inducing signaling complex. Cell **85:**817–827.
31. **Mykles, D. L.** 2001. Proteinase families and their inhibitors, p. 247–287. *In* L. M. Schwartz and J. D. Ashwell (ed.), Apoptosis. Academic Press, San Diego, Calif.
32. **Naides, S. J., L Scharosch, F. Foto, and E. Howard.** 1990. Rheumatologic manifestations of human parvovirus B19 infection in adults: initial two-year clinical experience. Arthritis Rheum. **33:**1297–1309.
33. **Naides, S. J. Y. V. Karetnyi, L. L. W. Cooling, R. S. Mark, and A. N. Langnas.** 1996. Human parvovirus B19 infection and hepatitis. Lancet **347:**1563.
34. **Naides, S. J.** 2000. Parvoviruses, p. 487–500. *In* S. Specter, R. L. Hodinka, and S. A. Young (ed.) Clinical virology manual, 3rd ed. Elsevier, New York, N.Y.
35. **Ozawa, K., G. Kurtzman, and N. Young.** 1986. Replication of the B19 parvovirus in human bone marrow cell cultures. Science **233:**883–886.
36. **Papadogiannakias, N., T. Tolfvenstam, B. Fischler, O. Norbeck, and K. Broliden.** 2002. Active, fulminant, lethal myocarditis associated with parvovirus B19 infection in an infant. Clin. Infect. Dis. **35:**1027–1031.
37. **Pardi, D. S., Y. Romero, L. E. Mertz, and D. D. Douglas.** Hepatitis-associated aplastic anemia and acute parvovirus B19 infection: a report of two cases and a review of the literature. Am. J. Gastroenterol. **93:**468–470.
38. **Pinho, J. R. R., V. A. F. Alves, A. F. Vieira, M. O. S. Moralez, L. E. P. Fonseca, B. Guz, A. Wakamatsu, E. I. R. Cançado, F. J. Carrilho, L. C. da Silva, A. P. Bernardini, and E. L. Durigon.** 2001. Detection of human parvovirus B19 in a patient with hepatitis. Brazilian J. Med. Biol. Res. **34:**1131–1138.
39. **Ponnazhagan, S., M. J. Woody, X.-S. Wang, S. Z. Zhou, and A. Srivastava.** 1995. Transcriptional transactivation of parvovirus B19 promoters in nonpermissive human cells by adenovirus type 2. J. Virol. **69:**8096–8101.

40. **Pörn-Ares, M. I., A. Samali, and S. Orrenius.** 1998. Cleavage of the calpain inhibitor, calpastatin, during apoptosis. Cell Death Differ. **5:**1028–1033.
41. **Schmidt, M., S. Afione, and R. Kotin.** 2000. Adeno-associated virus type 2 Rep 78 induces apoptosis through caspase activation independently of p53. J. Virol. **74:**9441–9450.
42. **Shan, Y.-S., P.-C. Lee, J.-R. Wang, H.-P. Tsai, C.-M. Sung, and Y.-T. Jin.** 2001. Fibrosing cholestatic hepatitis possibly related to persistent parvovirus B19 infection in a renal transplant recipient. Nephrol. Dial. Transplant. **16:**2420–2422.
43. **Söderlund, M., R. von Essen, J. Haapasaari, U. Kiistala, O. Kiviluoto, and K. Hedman.** Persistence of parvovirus B19 DNA in synovial membranes of young patients with and without chronic arthropathy. Lancet **349:**1063–1065.
44. **Sokal, E. M., M. Melchior, C. Cornu, A. T. Vandenbroucke, J. P. Buts, B. J. Cohen, and G. Burtonboy.** 1998. Acute parvovirus B19 infection associated with fulminant hepatitis of favorable prognosis in young children. Lancet **325:**1739–1741.
45. **Sol, N., J. Le Jünter, I. Vassias, J. M. Freyssinier, A. Thomas, A. F. Prigent, B. B. Rudkin, S. Fichelson, and F. Morinet.** 1999. Possible interactions between the NS-1 protein and tumor necrosis factor alpha pathways in erythroid cell apoptosis induced by human parvovirus B19. J. Virol. **73:**8762–8770.
46. **Stennicke, H. R., J. M. Jurgensmeier, H. Shin, Q. Deveraux, B. B. Wolf, X. Yang, Q. Zhou, H. M. Ellerby, L. M. Ellerby, D. Bredesen, D. R. Green, J. C. Reed, C. J. Froelich, and G. S. Salvesen.** 1998. Pro-caspase-3 is a major physiologic target of caspase-8. J. Biol. Chem. **273:**27084–27090.
47. **Thornberry, N. A., T. A. Rano, E. P. Peterson, D. M. Rasper, T. Timkey, M. Garcia-Calvo, V. M. Houtzager, P. A. Nordstrom, S. Roy, J. P. Vaillancourt, K. T. Chapman, and D. W. Nicholson.** 1997. A combinatorial approach defines specificities of members of the caspase family and granzyme B. Functional relationships established for key mediators of apoptosis. J. Biol. Chem. **272:**17907–17911.
48. **Tsuda, H.** 1993. Liver dysfunction caused by parvovirus B19. Am. J. Gastroenterol. **88:**1463.
49. **Tung, J., N. Hadzic, M. Layton, A. J. Baker, A. Dhawan, M. Rela, N. D. Heaton, and G. Mieli-Vergani.** 2001. Bone marrow failure in children with acute liver failure. J. Pediatr. Gastroenterol. Nutr. **31:**557–561.
50. **Wong, S., N. S. Young, and K. E. Brown.** 2003. Prevalence of parvovirus B19 in liver tissue: no association with fulminant hepatitis or hepatitis-associated aplastic anemia. J. Infect. Dis. **187:**1581–1586.
51. **Yoto, Y., T. Kudoh, K. Haseyama, N. Suzuki, and S. Chiba.** 1996. Human parvovirus B19 infection associated with acute hepatitis. Lancet **347:**868–869.